Desalination and Water Treatment
www.deswater.com
32 (2011) 351–356
August
1944-3994 / 1944-3986 © 2011 Desalination Publications. All rights reserved.
doi: 10.5004/dwt.2011.2721

A comparative study of phosphate removal technologies using adsorption and fluidized bed crystallization process

Yao-Hui Huang[a,b*], Yu-Jen Shih[a], Chun-Chi Chang[a], Shun-Hsing Chuang[c]

[a]*Department of Chemical Engineering, National Cheng Kung University, Tainan City 701, Taiwan*
Tel. +886 6 2757575 ext. 62636; email: yhhuang@mail.ncku.edu.tw
[b]*Resource Recycling and Management Research Center, National Cheng Kung University, Tainan City 701, Taiwan*
[c]*Chaoyang University of Technology, Department of Environmental Engineering and Management, Taichung County 41349, Taiwan*

Received 10 October 2010; Accepted in revised form 6 January 2011

ABSTRACT

This study compared the two novel technologies "calcium phosphate fluidized-bed crystallization (FBC) process" and "adsorption" which used an amorphous iron oxide BT-1 as the adsorbent for treating an industrial wastewater with high concentration of phosphate (1,000 mg P L^{-1}). In the adsorption process, most of phosphorus was adsorbed rapidly initially and then reached the thermodynamics equilibrium in 24 h. The phosphate adsorptive capacity of BT-1 was 2.03 mmole/g when the PO_4^{3-} equilibrium concentration was conditioned at 8.23 mM. The adsorption process followed the Langmuir and Temkin adsorption isotherm. In the FBC process, the optimum pH range was wider (pH > 5.3) for the total removal of phosphate than that for crystallization (optimum pH = 5.3–5.9). The total removal efficiency and crystallization ratio of phosphate were about 90% and 60%, respectively, in the optimum pH range. The EDS analysis showed that the Ca–P crystal products had an approximate 1:1:6 molar ratio of Ca:P:O. The XRD diagrams confirmed the crystal type of FBC product in a highly phosphate concentrated system was diacalcium phosphate dehydrate ($CaHPO_4 \cdot 2H_2O$, DCPD), which was different from the general calcium phosphate crystal content, hydroxyapatite ($Ca_5(PO_4)_3OH$, HAP), produced by FBC process.

Keywords: Fluidized bed crystallization; Adsorption; Phosphate removal; Hydroxylapatite; Dicalcium phosphate dehydrate

1. Introduction

Phosphate is one of the major causes of the water eutrophication, because it is often the limiting nutrient for primary production in fresh water and marine. Phosphate removal from the wastewater becomes the serious problem in recent years. It is also a topic gradually deeply concerned of countries all over the world. The world health organization (WHO) especially established the committee for this, in order to research its origin cause of formation and make the countermeasure.

Phosphate removal from wastewater has been widely investigated. For example, chemical precipitation, biological methods, crystallization, advanced chemical precipitation, ion exchange, magnetic, adsorption, tertiary, and sludge treatment [1,2]. Among them, biological method is widely accepted at industrial level but it needs high capital cost. Chemical precipitation is also widely used but it produces lots of chemical sludge. Consequently, the later research aim would tend to more competitive and

* Corresponding author.

Presented at the Third International Conference on Challenges in Environmental Science & Engineering, CESE-2010
26 September – 1 October 2010, The Sebel, Cairns, Queensland, Australia

economic technologies such as fluidized bed crystallization (FBC) and adsorption.

In the adsorption technology, the utilization of industrial wastes or byproducts for phosphorous removal has been given a great attention [3]. Those low cost adsorbents include fly ash [4–7], blast furnace slag [8,9], red mud [10–13], alum sludge [14,15], and other materials [16–23]. This study used an industrial waste-amorphous iron oxide (BT-1) which was produced by the fluidized-bed reactor Fenton (FBR-Fenton) as the adsorbent to treat phosphate wastewater. The source of the stock phosphate wastewater was obtained from the Al-etching procedure of a certain TFT-LCD factory in Taiwan. On the other hand, as the best of our knowledge, this is the first time to investigated calcium phosphate FBC technology in the treatment of such highly phosphate concentrated (1,000 mg P L^{-1}) in the word. The aim of this study is to find the optimum condition of pH value by FBC technology.

2. Materials and methods

2.1. Materials and analytical method

Stock solution of the phosphate wastewater was obtained from the Al-etching procedure of a certain TFT–LCD factory in Taiwan. Content of this wastewater included PO_4^{3-}, Cl^-, NO_3^-, SO_4^{2-}, and CH_3COO^-, etc. Working solutions were prepared to desire value by diluting the stock solution with D.I. water. All the experiment trails were carried out in the nature pH value of the diluted solution at 303 ± 2 K. The pH value is 2.1 ± 0.1. All other reagents used in the experiments were in analytical quality.

The BT-1 adsorbent was air-dried and then sieved to give a 0.25–0.50 mm size using standard sieves. The pH value was measured by standard method with 10g adsorbent placed in 20 ml of D.I. water. The BET surface area (m^2/g), micro-pore area (m^2/g), external surface area (m^2/g), total pore volume (cm^3/g), adsorption average pore diameter (A) were analyzed by surface area and porosity analyzer (Micromeritics ASAP 2010). Morphology of BT-1 was determined using a scanning electron microscope (SEM) (EOL JSM-6700F). As to the atomic composition, it was elucidated by energy dispersive spectra (EDS) spectrometer (Oxford INCA-400). The identification and crystallization of BT-1 was measured by X-ray diffraction (XRD) using a counter diffractometer (Rigaku RX III) with Cu Kα radiation. The accelerating voltage and current were 40 kV and 20 mA. The fraction of iron content was determined by atomic adsorption spectrophotometer (GBC Sens A) and undergoes the standard method. Phosphate concentration was measured by ion chromatography analysis (IC, 732 IC Detector, A Supp 1 column, Metrohm).

2.2. Experimental procedures

In the adsorption process, the surface of BT-1 absorbent was rinsed impurity or ash by clean water until the adsorbent has already cleaned completely. Then, the absorbent was dried at room temperature for more than 2 days. 1 L of 1,000 mg P L^{-1} solutions was treated with 1, 2, 5, 10 and 20 g of BT-1 adsorbent, respectively. Samples were kept for equilibration in a Jar-test isothermal reactor after 72 h. The temperature and the stirring speed were kept at 303 ± 2 K and 150 rpm. The changing amount of anion concentration in the solution with time was analyzed by ion chromatography analysis (IC).

On the other hand, the crystallization process was carried out in a FBR reactor (0.6 L) with a recycle pump for mixing (Fig. 1). The solution pH was adjusted by perchloric acid and sodium hydroxide using a pH meter (Action, A211). After predetermined quantity of SiO_2 support was put into the reactor, phosphate wastewater (1,000 mg P L^{-1}) and $CaCl_2$ solution with 2.0 molar ratio of Ca/P were pumped into the reactor and stirred with the recycle pump.

3. Results and discussion

3.1. The adsorption process

3.1.1. Adsorbent properties

The main compound of BT-1 adsorbent was iron oxide which was a disposable byproduct from the industrial FBR-Fenton reactor. Table 1 shows the physical properties of BT-1. The morphology of the SEM analysis showed in Fig. 2 compares the surface structure of BT-1 absorbent

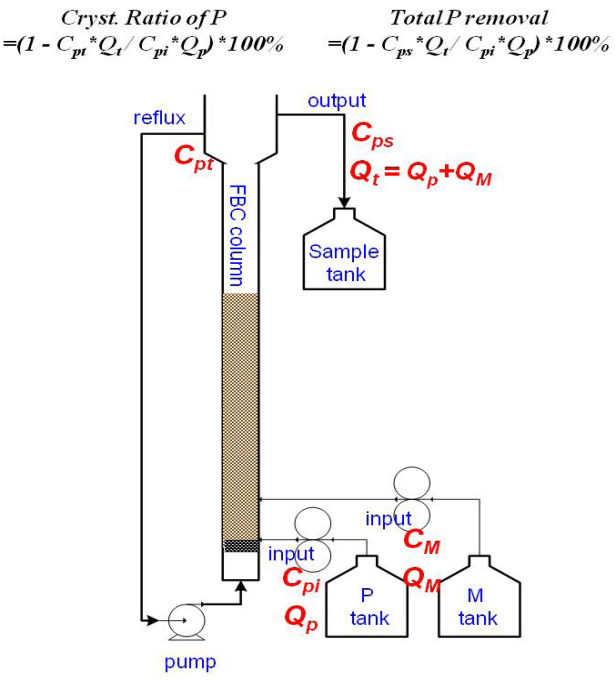

Fig. 1. Schematic diagram of a fluidized bed reactor.

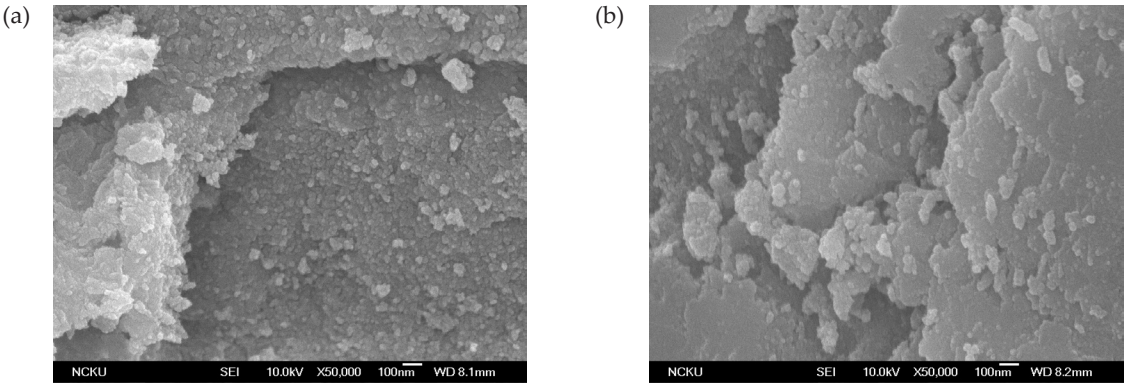

Fig. 2. SEM micrograph (5000×) of BT-1 before (a) and after (b) adsorption.

Table 1
Physical properties of BT-1 adsorbent

Properties	Value
Average particle size (μm)	500
pH	2.22
Bulk density	1.47
Particle density	3.17
BET surface area (m2/g)	178.23
Micro-pore area (m2/g)	25.57
External surface area (m2/g)	152.66
Total pore volume (cm3/g)	0.12
Adsorption average pore diameter (A)	27.23
Fraction of iron content (%)	0.45

Table 2
The EDS analysis of BT-1 before and after phosphate adsorption

Element	Before		After	
	Weight (%)	Atomic (%)	Weight (%)	Atomic (%)
C	4.56	11.05	3.24	7.38
O	31.99	58.2	36.64	62.62
S	1.39	1.26	1.18	1.01
Fe	54.39	28.34	43.18	20.65
Pt	7.67	1.14	8.68	1.22
P	—	—	8.01	7.12

before and after absorption process. Accordingly, the original BT-1 represented a lot of roughly structural breakage. It is rational to believe that this kind of porosity structure is the main reason of its high surface area and capability for phosphate adsorption. After adsorption process, a lot of irregular forms appeared in its surface structure and the morphology was observed slightly smoother.

The EDS data before and after adsorption are shown in Table 2. Before adsorption, no phosphorus content was observed, while the weight of phosphorus at the surface increased from 0% to 8.07% after adsorption. On the other hand, due to the very complicated composition of the working solution, this result also implied that BT-1 had selective ability in phosphate absorption.

3.1.2. Adsorptive capacity of BT-1 adsorbent

Fig. 3 shows the phosphorus removal percentages using BT-1 adsorbent increase dramatically in the first 8 h for 1, 2, 5, 10 and 20 g/L concentrations of BT-1, and reach to an equilibrium stage gradually at about 48 h.

The phosphate adsorptive capacity was calculated by Eq. (1):

$$q = (C_0 - C_e)/m_{ads} \quad (1)$$

where q is the phosphate adsorptive capacity at equilibrium (mmole/g), C_0 is initial phosphate concentration (mM), C_e is equilibrium phosphate concentration (mM) and m_{ads} is the dosage of adsorbent (g). The maximum phosphate adsorptive capacity of BT-1 in this study is 2.03 mmole/g at the 8.23 mM PO_4^{3-} equilibrium concentration.

3.1.3. Adsorptive model of BT-1 adsorbent for phosphate

The model of the phosphate adsorption isotherm experiments are shown in Fig. 4. Three isotherms, as described in Eqs. (2)–(4), were used for fitting the experimental data. The Freundlich isotherm model is an empirical equation based on the sorption occurred on a heterogeneous surface. It shows the relationship between the amount of phosphate adsorbed by the BT-1 adsorbent (mg g^{-1}) and the equilibrium concentration of phosphate (mg l^{-1}) in solution. It is given as:

$$qe = K_F C_e^{1/n} \quad (2)$$

where qe is the phosphate adsorptive capacity at equilibrium (mmole/g), C_e is equilibrium phosphate concentration (mM). The mechanism and the rate of adsorption are functions of the constants n and K_F. A value of n between

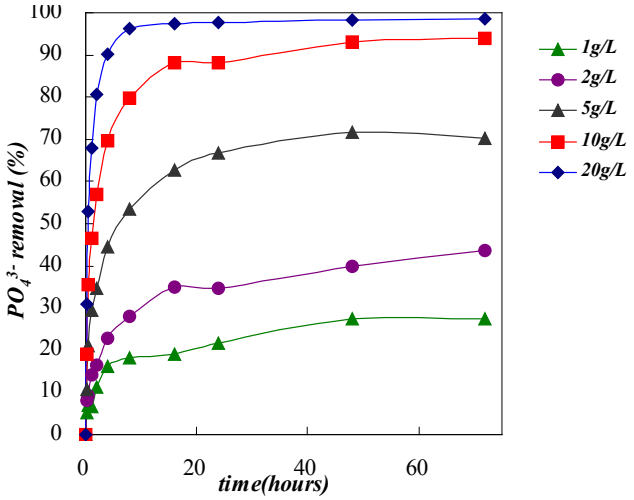

Fig. 3. Effect of BT-1 concentration on the phosphate removal.

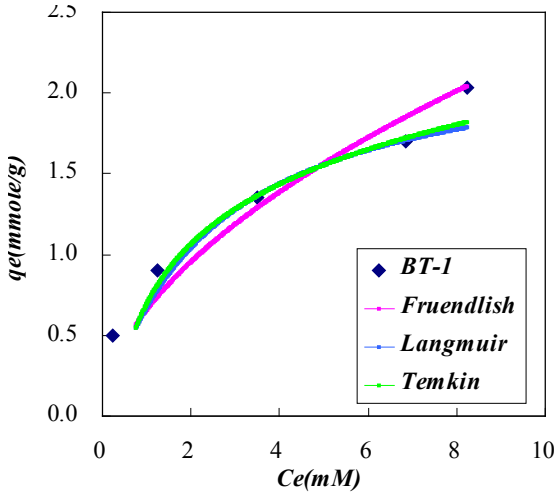

Fig. 4. Phosphate adsorption isotherm model (Fruendlich, Langmuir, Temkin) for BT-1.

1 to 10 means a good adsorbent used. The Freundlich equation can be linearized by taking logarithms and constants can be determined.

The most widely used isotherm equation for modeling the adsorption data is the Langmuir equation, which is valid for monolayer sorption onto a surface with a finite number of identical sites, and is given by Eq. (3).

$$qe = K_L q_m C_e / (1 + K_L C_e) \quad (3)$$

where K_L is the adsorption equilibrium constant represents the affinity of binding sites, and q_m is the maximum phosphate adsorptive capacity (mmol g^{-1}). The q_m and K_L can be determined from the linear plot of C_e/qe vs. C_e.

Temkin equation is given as:

$$qe = K_T + B \ln C_e \quad (4)$$

where K_T is the equilibrium binding constant corresponding to the maximum binding energy and constant B relates to the heat of adsorption.

Fig. 4 displays the qe vs. C_e plots and curve fittings for each isotherm, in which the values of K_F and n, K_L and q_m and K_T and B were calculated and listed in Table 3 along with associated correlation coefficients (R^2). It reveals that both the Langmuir and Temkin models have the better fittings than the Fruendlich model dose. According to these parameters, the BT-1 has a surface with high affinity for phosphate and is an excellent adsorbent used for adsorptive phosphate removal.

3.2. FBC technology

Fig. 5 illustrates the effect of pH on the concentration, total removal efficiency and crystal ratio of phosphate by FBC technology, respectively. The solution pH strongly affects the total removal efficiency of phosphate which increases with increasing pH and reaches to a plateau for pH > 5.3. About 95% of the maximum total removal efficiency of phosphate was obtained at pH 6.05. However, the crystallization ratio of phosphate shows different tendency. Although it also has a plateau for pH > 5.3, it dramatically decreases as pH > 5.9. The optimum pH range for crystallization is therefore from 5.3 to 5.9. In the optimum pH range, the total removal efficiency and crystallization ratio of phosphate are about 90% and 60%, respectively.

Table 3
Parameters of Fruendlich, Langmuir and Freundlich adsorption isotherm models for phosphate on BT-1 adsorbent

Freundlich		Langmuir		Temkin	
R^2	0.9148	R^2	0.9805	R^2	0.9844
K_F	0.6592	K_L	0.4102	K_T	3.7177
n	1.8619	q_m	2.3164	B	0.5321

EDS analysis (Fig. 6) shows that the molar ratio of Ca:P:O of FBC crystallized product approximates to 1:1:6, which was alluded to the XRD result (Fig. 7). The crystal type of FBC products was confirmed to be a diacalcium phosphate dehydrate ($CaHPO_4 \cdot 2H_2O$, DCPD) phase in this study. The DCPD phase may be the major species in a highly phosphate concentrated system, rather than the hydroxyapatite ($Ca_5(PO_4)_3OH$, HAP) in previous studies [24,25] which was generally produced in FBC process.

4. Conclusions

1. In adsorption process, BT-1 was demonstrated as an excellent phosphate adsorbent with adsorptive capac-

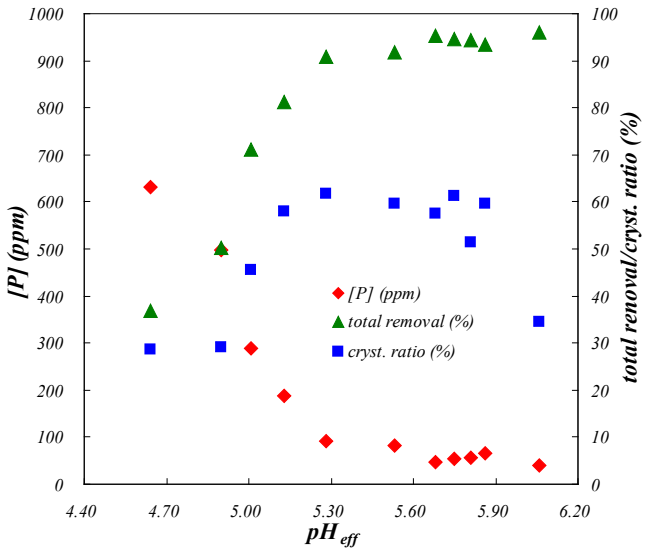

Fig. 5. Total removal and crystal ratio of phosphate with different pH values by FBC.

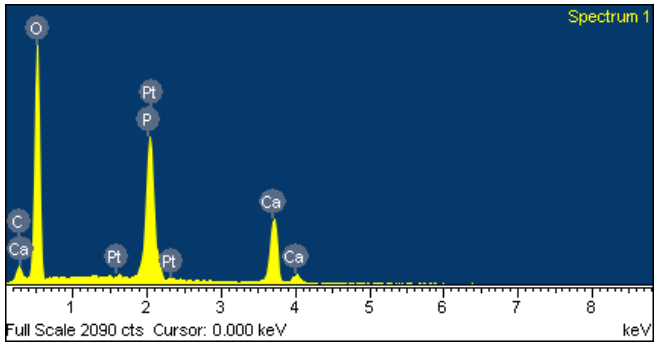

Element	Weight%	Atomic%
C K	2.88	5.55
O K	48.44	70.02
P K	14.99	11.19
Ca K	20.17	11.64
Pt M	13.52	1.60
Total	100.00	

Fig. 6 .The EDS data of Ca–P crystal.

ity of 2.03 mmole/g at the 8.23 mM PO_4^{3-} equilibrium concentration.

2. In FBC technology, it is suitable to deal with high concentration phosphorus waste water via heterogeneous crystallization. The crystallization ratio was over 60% for Ca/P = 2.0 and the 99% of phosphate removal was obtained as the optimum pH range 5.3–5.9. The species of crystallized product was evidenced to be a diacalcium phosphate dehydrate ($CaHPO_4{\cdot}2H_2O$, DCPD) phase.

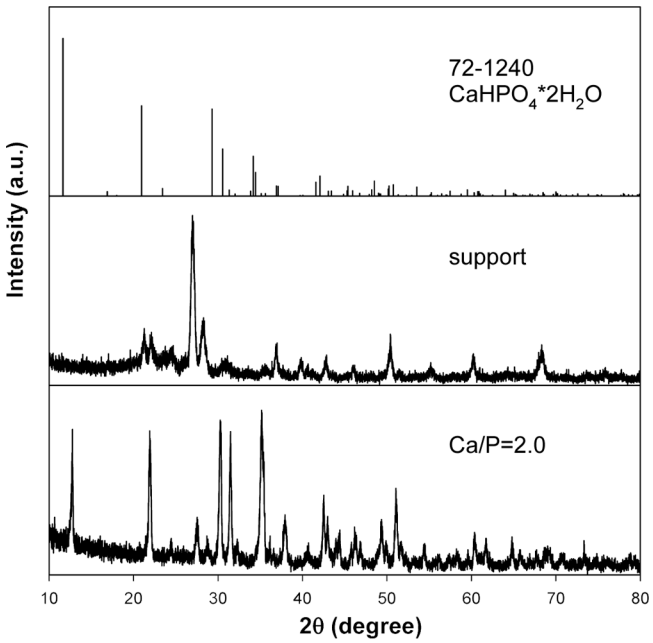

Fig. 7. The XRD diagram of support, Ca–P crystal and $CaHPO_4{\cdot}2H_2O$ standard material.

Acknowlegement

The authors thank the National Science Council of the Republic of China for financially supporting this research under Contract No. NSC98-2622-E-006 -014 -CC3.

References

[1] L.E. de-Bashan and Y. Bashan, Recent advances in removing phosphorus from wastewater and its future use as fertilizer (1997–2003), Wat. Res., 38(5) (2004) 1318–1326.
[2] G.K. Morse, S.W. Brett, J.A. Guy and J.N. Lester, Review: phosphorus removal and recovery technologies, Sci. Total Environ., 221(1) (1998) 69–81.
[3] L. Zeng, X. Li and J. Liu, Adsorptive removal of phosphate from aqueous solutions using iron oxide tailings, Wat. Res. 38(5) (2004) 1318–1326.
[4] K.C. Cheung and T.H. Venkitachalam, Improving phosphate removal of sand infiltration system using alkaline fly ash. Chemosphere, 41 (2000) 243–249.
[5] E. Yildiz, Phosphate removal from water by fly ash using cross-flow microfiltration, Sep. Purif. Technol., 35 (2004) 241–252.
[6] M.Y. Can and E. Yildiz, Phosphate removal from water by fly ash: Factorial experimental design, J. Hazard. Mater., 135 (2006) 165–170.
[7] J. Chena, H. Kong, D. Wua, Z. Hua, Z. Wanga and Y. Wang, Removal of phosphate from aqueous solution by zeolite synthesized from fly ash, J. Colloid Interf. Sci., 300(2) (2006) 491–497.
[8] L. Johansson and J.P. Gustafsson, Phosphate removal using blast furnace slags and opoka-mechanisms. Wat. Res., 34(1) (2000) 259–265.
[9] E. Oguz, Removal of phosphate from aqueous solution with blast furnace slag. J. Hazard. Mater., 114 (2004) 131–137.
[10] B. Koumanova, M. Drame and M. Popangelova, Phosphate removal from aqueous solutions using red mud wasted in bauxite Bayer's process. Resour. Conserv. Recy., 19 (1997) 11–20.

[11] G. Akay, B. Keskinler, A. Çakici and U. Danis, Phosphate removal from water by red mud using crossflow microfiltration, Wat. Res., 32(3) (1998) 717–726.
[12] Y. Li, C. Liu, Z. Luan, X. Peng, C. Zhu, Z. Chen, Z. Zhang, J. Fan and Z. Jia, Phosphate removal from aqueous solutions using raw and activated red mud and fly ash, J. Hazard. Mater., 137 (2006) 374–383.
[13] C. Liu, Y. Li, Z. Luan, Z. Chen, Z. Zhang and Z. Jia, Adsorption removal of phosphate from aqueous solution by active red mud, J. Environ. Sci., 19(10) (2007) 1166–1170.
[14] S.H. Huang and B. Chiswell, Phosphate removal from wastewater using spent alum sludge. Wat. Sci. Technol., 42(3) (2000) 295–300.
[15] S.M. Lee, B.J. Choi and K.H. Kim, Removal of phosphate by seafood processing wasted sludge, Wat. Sci. Technol., 46(9) (2002) 297–302.
[16] E. Oguz, A. Gurses and M. Yalcin, Removal of phosphate from waste waters by adsorption, Wat. Air Soil Poll., 148 (2003) 279–287.
[17] S. Tanada, M. Kabayama, N. Kawasaki, T. Sakiyama, T. Nakamura, M. Araki and T. Tamura, Removal of phosphate by aluminum oxide hydroxide, J. Colloid Interf. Sci., 257(1) (2003) 135–140.
[18] C. Namasivayam, A. Sakoda and M. Suzuki, Removal of phosphate by adsorption onto oyster shell powder-Kinetic studies, J. Chem. Technol. Biot., 80(3) (2005) 356–358.
[19] S. Karaca, A. Gürses, M. Ejder and M. Açıkyıldız, Adsorptive removal of phosphate from aqueous solutions using raw and calcinated dolomite, J. Hazard. Mater., 128 (2006) 273–279.
[20] M.S. Onyango, D. Kuchar, M. Kubota and H. Matsuda, Adsorptive removal of phosphate ions from aqueous solution using synthetic zeolite, Ind. Eng. Chem. Res., 46(3) (2007) 894–900.
[21] Y.H. Moon, J.G. Kim, J.S. Ahn, G.H. Lee and H.S. Moon, Phosphate removal using sludge from fuller's earth production, J. Hazard. Mater., 143 (2007) 41–48.
[22] S.L. Wang, C.Y. Cheng, Y.M. Tzou, R.B. Liaw, T.W. Chang and J.H. Chen, Phosphate removal from water using lithium intercalated gibbsite, J. Hazard. Mater., 147 (2007) 205–212.
[23] K. Karageorgiou, M. Paschalis and G.N. Anastassakis, Removal of phosphate species from solution by adsorption onto calcite used as natural adsorbent, J. Hazard. Mater., 139 (2007) 447–452.
[24] J. Wang, Y. Song, P. Yuan, J. Peng and M. Fan Modeling the crystallization of magnesium ammonium phosphate for phosphorus recovery, Chemosphere, 65(7) (2006) 1182–1187.
[25] H. Jang and S.H. Kang, Phosphorus removal using cow bone in hydroxyapatite crystallization, Wat. Res., 36(5) (2002) 1324–1330.